

# Impact of Feedback Delays on EESM-based Wideband Link Adaptation: Modeling and Analysis

Jobin Francis and Neelesh B. Mehta, *Senior Member, IEEE*

**Abstract**—In orthogonal frequency division multiplexing (OFDM) systems, such as long term evolution (LTE) and WiMAX, a codeword is transmitted over a group of subcarriers. Since the subcarriers see different channel gains in a frequency-selective channel, the modulation and coding scheme (MCS) of the codeword must be selected based on the vector of signal-to-noise-ratios (SNRs) of these subcarriers. Exponential effective SNR mapping (EESM) simplifies this problem by mapping the vector of SNRs into a single, equivalent flat-fading SNR. We develop a new analytical framework to characterize the throughput of EESM-based rate adaptation in such wideband channels in the presence of feedback delays, which make the choice of the MCS partially outdated by the time data transmission takes place. To this end, we first propose a novel bivariate gamma distribution to model the joint statistics of EESM at the times of estimation and data transmission. We then derive a novel expression for the throughput as a function of feedback delay. Our framework works for both correlated and independent subcarriers and for various multiple antenna diversity modes, and is accurate over a wide range of delays.

## I. INTRODUCTION

Next generation wireless systems, such as long term evolution (LTE) and WiMAX, have been designed to meet the ever growing demand for higher data rates. In these systems, orthogonal frequency division multiplexing (OFDM) is the physical layer access technology of choice because it avoids inter-symbol and intra-cell interference. OFDM divides the available bandwidth into narrowband orthogonal subcarriers. To efficiently utilize the scarce bandwidth, adaptive modulation and coding (AMC), in which rate is adapted based on the channel state information (CSI), is used.

In these OFDM systems, a codeword is transmitted over a group of subcarriers. Due to the frequency-selective nature of the channel, different subcarriers see different gains. In general, this depends on the number of subcarriers assigned to the codeword and the power-delay profile of the channel. Thus, the AMC scheme must select the modulation and coding scheme (MCS) based on the vector of signal-to-noise ratios (SNRs) of the subcarriers to be assigned to the codeword. This is unlike the well studied AMC over narrowband channels, in which the MCS choice is based on just one SNR [1].

A practical issue that arises in such systems is feedback delay, which is due to the delay between the time of estimation of the channel gains and the time of data transmission. This

delay is of the order of milliseconds or tens of milliseconds [2]. It degrades the throughput for two reasons. Firstly, the AMC scheme may overestimate the rate the channel can support, which results in an outage because the transmitted codeword cannot be decoded correctly. Secondly, the AMC scheme may underestimate the rate resulting in a lower spectral efficiency.

## A. Related Literature

We now present a brief survey of the prior works on adaptation in OFDM systems with and without feedback delay.

In [3], the performance of an OFDM system with various feedback reduction schemes, frequency-domain scheduling, and feedback delay is analyzed. However, in it, the frequency response is assumed to be flat across a resource block (RB), which is the basic scheduling and feedback unit. Although multiple RBs can be allotted to a user, no coding across RBs is assumed. Hence, the rate adaptation model is similar to that for narrowband fading. The effect of channel estimation errors, quantization errors, feedback errors, and feedback delay on throughput is analyzed in [4]. In it, the rate for every subcarrier is assumed to be adaptable. Consequently, the rate adaptation model is similar to that in narrowband channels. A similar subcarrier-specific adaptation with feedback delays is also considered in [5], [6].

*LQM-based Adaptation:* In order to simplify the problem of link adaptation over wideband fading channels, link quality metrics (LQMs) such as exponential effective SNR mapping (EESM) have been proposed [7]–[9]. EESM maps the vector of subcarrier SNRs seen by the codeword into an effective flat-fading SNR, which is interpreted to be the equivalent SNR in an additive white Gaussian noise (AWGN) channel. If  $\gamma_i(t)$  denotes the SNR of the  $i^{\text{th}}$  subcarrier at time  $t$ , for  $1 \leq i \leq N_{\text{sc}}$ , then the effective SNR  $\gamma_{\text{eff}}^{(m)}(t)$  for MCS  $m$  is defined as

$$\gamma_{\text{eff}}^{(m)}(t) = -\beta_m \log \left( \frac{1}{N_{\text{sc}}} \sum_{i=1}^{N_{\text{sc}}} \exp \left( -\frac{\gamma_i(t)}{\beta_m} \right) \right), \quad (1)$$

where  $\beta_m > 0$  is an MCS-dependent parameter. The accuracy of EESM has been established in several prior works [8], [9]. Thus, EESM reduces the problem of AMC over a frequency-selective channel to that over a frequency-flat channel. The relevance of EESM can be gauged from its usage in system-level simulations of LTE and WiMAX [10], [11], and in generating feedback to the transmitter for link adaptation and scheduling [12].

While LQM-based link adaptation is studied in [13], [14], feedback delay is ignored and only Monte Carlo simulation results are presented. While [12] considers EESM-based

The authors are with the Dept. of Electrical Communication Eng. at the Indian Institute of Science (IISc), Bangalore, India.

Emails: jobin@ece.iisc.ernet.in, nbmehta@ece.iisc.ernet.in.

This work is partly supported by a philanthropic grant from the Broadcom Foundation, USA and a research grant from DST, India and EPSRC, UK under the auspices of the India-UK Advanced Technology Center (IU-ATC).

feedback and frequency-domain scheduling, it uses a sub-optimal AMC scheme and ignores feedback delay. Closed-form expressions for the throughput of EESM-based AMC are derived in [15], but feedback delay is not accounted for. A simulation study of the impact of feedback delay when mutual-information effective SNR mapping (MI-ESM) is used as the LQM is presented in [7].

From the papers above, we see that the effect of feedback delay in the practically important case in which the MCS is adapted for a codeword that is transmitted over multiple subcarriers that see different, albeit correlated gains, has not been analyzed. With feedback delays, the joint or bivariate distribution of the effective SNRs  $\gamma_{\text{eff}}^{(m_1)}(t)$  and  $\gamma_{\text{eff}}^{(m_2)}(t + \tau)$ , each of which is a non-linear mapping of subcarrier SNRs, is needed. This is because the MCS  $m_1$  is decided at time  $t$  on the basis of  $\gamma_{\text{eff}}^{(1)}(t), \dots, \gamma_{\text{eff}}^{(L)}(t)$ , where  $L$  is the number of MCSs available to choose from, while the success of the transmission depends on  $\gamma_{\text{eff}}^{(m_1)}(t + \tau)$ .

However, the approximations that have been proposed in [15], [16] for the marginal (one-dimensional) distribution of EESM do not easily generalize to the bivariate case. Specifically, for the beta model proposed in [15], no tractable, natural extension to the bivariate case exists in the literature. The generalized extreme value (GEV) and Pearson models proposed in [16] also face the same problem. Thus, an altogether new approach is needed to overcome these shortcomings.

Another issue with the model in [12] is that EESM is an MCS-dependent mapping because the parameter  $\beta_m$  is different for different MCSs. For example, in LTE, it varies from 1.0 for QPSK with rate 0.08 code to 28.9 for 64-QAM with rate 0.93 code [17]. Thus, even with EESM, the MCS has to be decided based on multiple EESM values, one for each MCS. These are correlated because they are obtained from the same vector of subcarrier SNRs.

## B. Contributions

Our goal is to analyze the effect of feedback delay on the throughput of EESM-based AMC in a point-to-point wideband link with fading. To this end, we first model the random variables (RVs)  $\gamma_{\text{eff}}^{(m)}(t)$  and  $\gamma_{\text{eff}}^{(m)}(t + \tau)$  with a bivariate gamma distribution [18]. To the best of our knowledge, this is the first bivariate statistical characterization of EESM. The choice of the distribution is motivated by the observation that at very high correlations,  $\gamma_{\text{eff}}^{(m)}(t) \approx \gamma_i(t)$ , for any  $1 \leq i \leq N_{\text{sc}}$ , which is a gamma distributed RV. The same holds at time  $t + \tau$ . We shall see that the bivariate gamma distribution is accurate even for independent subcarriers.

The bivariate gamma distribution is specified by four parameters, which are determined using a new moment generating function (MGF)-matching method, which is uniquely well-suited for EESM. Specifically, given the functional form of EESM in (1), we show that its MGF can be evaluated in a simple closed-form at certain specific points, unlike its moments that often require cumbersome Monte Carlo simulations [12].

The proposed bivariate gamma model for EESM is then used to obtain a novel expression for the AMC throughput with

feedback delays. The analysis is accurate and quite general in that it covers multiple antenna modes and easily accounts for any correlation among the subcarriers.

## C. Organization and Notation

The system model is given in Section II. The bivariate EESM model and the throughput analysis are developed in Section III. Simulation results are presented in Section IV, and are followed by our conclusions in Section V.

We denote the transpose of a matrix  $\mathbf{A}$  by  $\mathbf{A}^T$ . Let  $c^*$  and  $|c|$  respectively denote the complex conjugate and the absolute value of the complex number  $c$ . Let  $\mathbb{E}[X]$ ,  $F_X(x)$ , and  $f_X(x)$  denote the expectation, the cumulative distribution function (CDF), and the probability density function (PDF) of the RV  $X$ , respectively. The MGF  $\Psi_X(z)$  of  $X$  is defined as  $\mathbb{E}[\exp(-zX)]$ . For two RVs  $X$  and  $Y$ , the conditional PDF of  $Y$  given  $X = x$  is denoted by  $f_Y(y|x)$ .

## II. WIDEBAND ADAPTATION MODEL

We consider a point-to-point OFDM link with  $N_t$  transmit antennas,  $N_r$  receive antennas, and frequency-selective fading. The transmitted codeword is encoded across  $N_{\text{sc}}$  subcarriers. Based on the estimated channel gains on these subcarriers, the receiver selects an MCS. The selected MCS is then fed back to the transmitter. For example, in LTE one among 16 different MCSs is fed back [2].

### A. Channel Model

Let  $h_{kl}^{(i)}(t)$  denote the complex channel gain between the  $k^{\text{th}}$  receive antenna and the  $l^{\text{th}}$  transmit antenna of the  $i^{\text{th}}$  subcarrier at time  $t$ . It is a circularly symmetric complex Gaussian RV with unit variance. Let  $\tau$  denote the delay between the times of channel estimation and data transmission. As per the Jakes' fading model [1],  $h_{kl}^{(i)}(t)$  and  $h_{kl}^{(i)}(t + \tau)$  are jointly Gaussian with correlation coefficient  $\rho(\tau) = J_0(2\pi f_d \tau)$ , where  $f_d$  is the Doppler spread and  $J_0(\cdot)$  is the zeroth-order Bessel function of the first kind [19]. Notice that  $f_d$  and  $\tau$  always appear in the form of a product  $f_d \tau$ , which we shall refer to as the *normalized delay*. The channel estimates at the receiver are assumed to be perfect, as assumed in [7], [13].

The complex channel gains on different transmit-recvie (Tx-Rx) antenna pairs are assumed to be identical and independently distributed. This is justified in a rich scattering environment when the antennas are spaced sufficiently far apart. Thus, the channel gain vector of the  $(k, l)^{\text{th}}$  antenna pair at time  $t$ ,  $\mathbf{h}_{kl}(t) = [h_{kl}^{(1)}(t), h_{kl}^{(2)}(t), \dots, h_{kl}^{(N_{\text{sc}})}(t)]^T$ , is a circularly symmetric complex Gaussian random vector with covariance matrix  $\mathbf{C}$ , whose  $(i, j)^{\text{th}}$  element is  $C_{ij} = \mathbb{E}[h_{kl}^{(i)}(t)h_{kl}^{(j)*}(t)]$ .

Let  $\sigma^2$  denote the average SNR of a Tx-Rx link. The SNR  $\gamma_i(t)$  of the  $i^{\text{th}}$  subcarrier at time  $t$  depends on the multiple antenna mode. Specifically, for single-input-single-output (SISO), i.e.,  $N_t = N_r = 1$ , it is  $\gamma_i(t) = \sigma^2 |h_{11}^{(i)}(t)|^2$ . For single-input-multiple-output (SIMO) with  $N_t = 1$ ,  $N_r > 1$  and maximal ratio combining (MRC), it is  $\gamma_i(t) = \sigma^2 \sum_{k=1}^{N_r} |h_{k1}^{(i)}(t)|^2$ . Similarly, for multiple-input-single-output (MISO) with  $N_t > 1$ ,  $N_r = 1$  and maximal

ratio transmission (MRT), it is  $\gamma_i(t) = \sigma^2 \sum_{l=1}^{N_t} |h_{1l}^{(i)}(t)|^2$ . In each of these cases, the subcarrier SNR can be written as  $\gamma_i(t) = aX_D^{(i)}(t)$ , where  $a$  is a scaling constant and  $X_D^{(i)}(t)$  is a Chi-squared RV with  $D$  degrees-of-freedom. Specifically,  $a = \frac{\sigma^2}{2}$  and  $D = 2$  for SISO,  $a = \frac{\sigma^2}{2}$  and  $D = 2N_r$  for SIMO, and  $a = \frac{\sigma^2}{2}$  and  $D = 2N_t$  for MISO. For multiple-input-multiple-output (MIMO) that uses spatial multiplexing and a zero-forcing receiver,  $a = \frac{\sigma^2}{2}$  and  $D = 2(N_r - N_t + 1)$  [1].<sup>1</sup>

### B. EESM-based AMC

We focus on the practical case of discrete rate adaptation [1], [2]. Let  $r_m$  denote the rate of MCS  $m$ . The  $L$  MCSs are indexed in the increasing order of their rates, i.e.,  $0 < r_1 \leq r_2 \leq \dots \leq r_L$ . The AMC scheme selects an MCS to maximize the throughput while ensuring that the instantaneous block error rate (BLER) is less than or equal to a target value  $\text{BLER}_t$  [2], [7], [15].

Using EESM, for any MCS, the instantaneous BLER constraint can be transformed into an equivalent constraint on the BLER in an AWGN channel. Let  $\text{BLER}_{\text{AWGN}}(\cdot, m)$  denote the BLER in an AWGN channel for MCS  $m$ . Then, MCS  $m$  satisfies the instantaneous BLER constraint if its effective SNR at the time of transmission exceeds  $T_m$ , where  $\text{BLER}_{\text{AWGN}}(T_m, m) = \text{BLER}_t$ . Here, we have implicitly assumed that EESM-based BLER estimates are perfect. This is justified because, as shown in [8], [9], EESM is accurate.

The AMC scheme proceeds as follows [7], [14], [15]. It chooses the highest rate MCS at time  $t$  if  $\gamma_{\text{eff}}^{(L)}(t) \geq T_L$ . Else, the scheme moves to the next highest MCS, and so on. If  $\gamma_{\text{eff}}^{(i)}(t) < T_i$ , for all  $i = 1, \dots, L$ , then no data transmission takes place because the BLER constraint cannot be satisfied.

### C. Throughput Analysis: Preliminaries

Let  $m_{\text{opt}}(t) \in \{1, \dots, L\}$  denote the MCS selected at time  $t$ . The transmission with this MCS, which occurs at time  $t + \tau$ , will be successful if  $\gamma_{\text{eff}}^{(m_{\text{opt}}(t))}(t + \tau) \geq T_{m_{\text{opt}}(t)}$ . Thus, the average throughput  $\bar{R}(\tau)$  is given by<sup>2</sup>

$$\bar{R}(\tau) = \sum_{m=1}^L r_m \Pr \left\{ m_{\text{opt}}(t) = m, \gamma_{\text{eff}}^{(m)}(t + \tau) \geq T_m \right\}. \quad (2)$$

MCS  $m$  is selected if its EESM is greater than or equal to  $T_m$  and the EESM values of the higher rate MCSs are less than their SNR thresholds. Thus,

$$\Pr \left\{ m_{\text{opt}}(t) = m, \gamma_{\text{eff}}^{(m)}(t + \tau) \geq T_m \right\} = P \left( \gamma_{\text{eff}}^{(m)}(t) \geq T_m, \gamma_{\text{eff}}^{(m+1)}(t) < T_{m+1}, \dots, \gamma_{\text{eff}}^{(L)}(t) < T_L, \gamma_{\text{eff}}^{(m)}(t + \tau) \geq T_m \right). \quad (3)$$

<sup>1</sup>In order to focus on the impact of feedback delays on wideband rate adaptation, we do not include in our model the outdated nature of the transmit beamforming weights [20], which are used in MISO and MIMO. Note, however, that this limitation does not apply to SIMO and open-loop MISO.

<sup>2</sup>For tractability, we assume an outage-based model, i.e., the BLER in an AWGN channel is approximated as a step function. This assumption is reasonable because with advanced coding schemes the BLER falls exponentially with the SNR.

The  $(L - m + 2)$ -dimensional joint distribution of the correlated RVs  $\gamma_{\text{eff}}^{(m)}(t), \gamma_{\text{eff}}^{(m+1)}(t), \dots, \gamma_{\text{eff}}^{(L)}(t)$ , and  $\gamma_{\text{eff}}^{(m)}(t + \tau)$  is required to evaluate (3), but no closed-form for it is available. We circumvent this problem by using the following approximation, which is derived in Appendix A and is verified to be accurate in Section IV-B.

$$\begin{aligned} \Pr \left\{ m_{\text{opt}}(t) = m, \gamma_{\text{eff}}^{(m)}(t + \tau) \geq T_m \right\} \\ \approx P \left( \gamma_{\text{eff}}^{(m)}(t) \geq T_m, \gamma_{\text{eff}}^{(m)}(t + \tau) \geq T_m \right) \\ - P \left( \gamma_{\text{eff}}^{(m+1)}(t) \geq T_{m+1}, \gamma_{\text{eff}}^{(m)}(t + \tau) \geq T_m \right). \quad (4) \end{aligned}$$

### III. EESM EVOLUTION MODEL AND THROUGHPUT ANALYSIS

We see from (4) that the bivariate distributions of  $\gamma_{\text{eff}}^{(m)}(t)$  and  $\gamma_{\text{eff}}^{(m)}(t + \tau)$ , and  $\gamma_{\text{eff}}^{(m+1)}(t)$  and  $\gamma_{\text{eff}}^{(m)}(t + \tau)$  are needed. For this, we propose a new bivariate gamma distribution [18] for modeling in a tractable manner the joint distribution of the RVs  $\gamma_{\text{eff}}^{(m_1)}(t)$  and  $\gamma_{\text{eff}}^{(m_2)}(t + \tau)$ , whose motivation was given in Section I-B.

#### A. Bivariate Gamma Distribution: Preliminaries

We summarize the key properties of this distribution below. Let the RVs  $U$  and  $V$  be bivariate gamma RVs. Their bivariate PDF is given in terms of four parameters  $q, s, p$ , and  $r$  as

$$\begin{aligned} f_{U,V}(u, v) = \frac{1}{r\Gamma(q)} \exp \left( -\frac{pu + sv}{r} \right) \left( \frac{uv}{sp - r} \right)^{\frac{q-1}{2}} \\ \times I_{q-1} \left( \frac{2\sqrt{uv(sp - r)}}{r} \right), \quad u > 0, v > 0, \quad (5) \end{aligned}$$

where  $q \geq 0, s > 0, p > 0, 0 < r \leq sp, \Gamma(\cdot)$  is the gamma function, and  $I_{q-1}(\cdot)$  is the  $(q - 1)$ <sup>th</sup>-order modified Bessel function of first kind [19]. The bivariate CDF is given by

$$\begin{aligned} F_{U,V}(u, v) = \frac{r^q}{\Gamma(q)} \sum_{k=0}^{\infty} \frac{(sp - r)^k \Gamma(k + q)}{k!(sp)^{k+q}} \\ \times \Gamma_{\text{inc}} \left( k + q, u \frac{p}{r} \right) \Gamma_{\text{inc}} \left( k + q, v \frac{s}{r} \right), \quad u > 0, v > 0, \quad (6) \end{aligned}$$

where  $\Gamma_{\text{inc}}(q, a) = \frac{1}{\Gamma(q)} \int_0^a x^{q-1} \exp(-x) dx$  is the incomplete gamma function and  $B(\cdot, \cdot)$  is the beta function [19].

The RVs  $U$  and  $V$  are gamma distributed with parameters  $q$  and  $s$ , and  $q$  and  $p$ , respectively. Their PDFs are given in [18]. Further, the conditional CDF  $F_V(v|u)$  of  $V$  given  $U = u$  is

$$\begin{aligned} F_V(v|u) = \exp \left( -u \frac{sp - r}{sr} \right) \sum_{k=0}^{\infty} \frac{u^k}{k!} \left( \frac{sp - r}{sr} \right)^k \\ \times \Gamma_{\text{inc}} \left( k + q, \frac{sv}{r} \right), \quad u > 0, v > 0. \quad (7) \end{aligned}$$

Finally, the joint MGF of  $U$  and  $V$  is given as follows:

$$\Psi_{U,V}(z_1, z_2) = (1 + sz_1 + pz_2 + rz_1z_2)^{-q}. \quad (8)$$

1) *Computing the Bivariate Gamma Parameters:* Since we are interested in the joint PDF of  $\gamma_{\text{eff}}^{(m_1)}(t)$  and  $\gamma_{\text{eff}}^{(m_2)}(t + \tau)$ , we introduce subscripts  $m_1$  and  $m_2$  into the four distribution parameters and denote them as  $q_{m_1, m_2}$ ,  $s_{m_1, m_2}$ ,  $p_{m_1, m_2}$ , and  $r_{m_1, m_2}$ . These must be expressed in terms of the system parameters  $a$ ,  $D$ ,  $N_{\text{sc}}$ , and  $\mathbf{C}$  in order to specify the bivariate gamma PDF. We do this by matching the joint MGF of the RVs  $\gamma_{\text{eff}}^{(m_1)}(t)$  and  $\gamma_{\text{eff}}^{(m_2)}(t + \tau)$  with that of the bivariate gamma distribution at four carefully chosen points as follows.

Let  $Y_m(t) = \frac{1}{N_{\text{sc}}} \sum_{i=1}^{N_{\text{sc}}} e^{-\frac{\gamma_i(t)}{\beta_m}}$ . Therefore,  $\Psi_{\gamma_{\text{eff}}^{(m)}}(z) = \mathbb{E} \left[ (Y_m(t))^{z\beta_m} \right]$ . From this and (8), we get

$$\begin{aligned} \mathbb{E} [Y_{m_1}(t)] &= \Psi_{\gamma_{\text{eff}}^{(m_1)}(t), \gamma_{\text{eff}}^{(m_2)}(t+\tau)}(\beta_{m_1}^{-1}, 0) \\ &= (1 + s_{m_1, m_2} \beta_{m_1}^{-1})^{-q_{m_1, m_2}}, \end{aligned} \quad (9)$$

$$\begin{aligned} \mathbb{E} [Y_{m_1}^2(t)] &= \Psi_{\gamma_{\text{eff}}^{(m_1)}(t), \gamma_{\text{eff}}^{(m_2)}(t+\tau)}(2\beta_{m_1}^{-1}, 0) \\ &= (1 + 2s_{m_1, m_2} \beta_{m_1}^{-1})^{-q_{m_1, m_2}}, \end{aligned} \quad (10)$$

$$\begin{aligned} \mathbb{E} [Y_{m_2}(t)] &= \Psi_{\gamma_{\text{eff}}^{(m_1)}(t), \gamma_{\text{eff}}^{(m_2)}(t+\tau)}(0, \beta_{m_2}^{-1}) \\ &= (1 + p_{m_1, m_2} \beta_{m_2}^{-1})^{-q_{m_1, m_2}}, \end{aligned} \quad (11)$$

$$\begin{aligned} \mathbb{E} [Y_{m_1}(t)Y_{m_2}(t + \tau)] &= \Psi_{\gamma_{\text{eff}}^{(m_1)}(t), \gamma_{\text{eff}}^{(m_2)}(t+\tau)}(\beta_{m_1}^{-1}, \beta_{m_2}^{-1}) \\ &= (1 + s_{m_1, m_2} \beta_{m_1}^{-1} + p_{m_1, m_2} \beta_{m_2}^{-1} + r_{m_1, m_2} \beta_{m_1}^{-1} \beta_{m_2}^{-1})^{-q_{m_1, m_2}}. \end{aligned} \quad (12)$$

From (9) and (10), we obtain the following non-linear equation:  $1 + 2\beta_{m_1}^{-1}s_{m_1, m_2} = (1 + \beta_{m_1}^{-1}s_{m_1, m_2})^\delta$ , where  $\delta = \frac{\log(\mathbb{E}[Y_{m_1}^2(t)])}{\log(\mathbb{E}[Y_{m_1}(t)])} > 1$ . It can be shown that the above equation has a unique non-zero solution, which is the desired value of  $s_{m_1, m_2}$ . It is computed numerically. Given  $s_{m_1, m_2}$ , the remaining parameters can be written in closed-form from (10), (11), and (12) as follows:<sup>3</sup>

$$q_{m_1, m_2} = -\frac{\log(\mathbb{E}[Y_{m_1}(t)])}{\log(1 + \beta_{m_1}^{-1}s_{m_1, m_2})}, \quad (13)$$

$$p_{m_1, m_2} = \beta_{m_2} (\mathbb{E}[Y_{m_2}(t)])^{-\frac{1}{q_{m_1, m_2}}} - \beta_{m_2}, \quad (14)$$

$$\begin{aligned} r_{m_1, m_2} &= \beta_{m_1} \beta_{m_2} (\mathbb{E}[Y_{m_1}(t)Y_{m_2}(t + \tau)])^{-\frac{1}{q_{m_1, m_2}}} \\ &\quad - \beta_{m_1} p_{m_1, m_2} - \beta_{m_2} s_{m_1, m_2} - \beta_{m_1} \beta_{m_2}. \end{aligned} \quad (15)$$

2) *Moments of  $Y_{m_1}(t)$  and  $Y_{m_2}(t + \tau)$ :* Thus, all that remains to be done is to compute the moments  $\mathbb{E}[Y_{m_1}(t)]$ ,  $\mathbb{E}[Y_{m_2}(t)]$ ,  $\mathbb{E}[Y_{m_1}^2(t)]$ , and  $\mathbb{E}[Y_{m_1}(t)Y_{m_2}(t + \tau)]$ . These are given in closed-form below, which applies to any subcarrier correlation matrix  $\mathbf{C}$ .

**Result 1:** The first two moments of  $Y_m(t)$  are given by

$$\mathbb{E}[Y_m(t)] = (1 + 2a\beta_m^{-1})^{-\frac{D}{2}}, \quad (16)$$

$$\begin{aligned} \mathbb{E}[Y_m^2(t)] &= \frac{1}{N_{\text{sc}}^2} \sum_{i=1}^{N_{\text{sc}}} \sum_{j=1}^{N_{\text{sc}}} \left[ (1 + 2a\beta_m^{-1})^2 \right. \\ &\quad \left. - 4a^2 |C_{ij}|^2 \beta_m^{-2} \right]^{-\frac{D}{2}}, \quad m = m_1, m_2, \end{aligned} \quad (17)$$

<sup>3</sup>In (9), (10), (11), and (12), the ordering of the RVs matters in determining the parameters. In case  $r_{m_1, m_2}$  turns out to be negative, we compute the parameters of  $(\gamma_{\text{eff}}^{(m_2)}(t + \tau), \gamma_{\text{eff}}^{(m_1)}(t))$  instead.

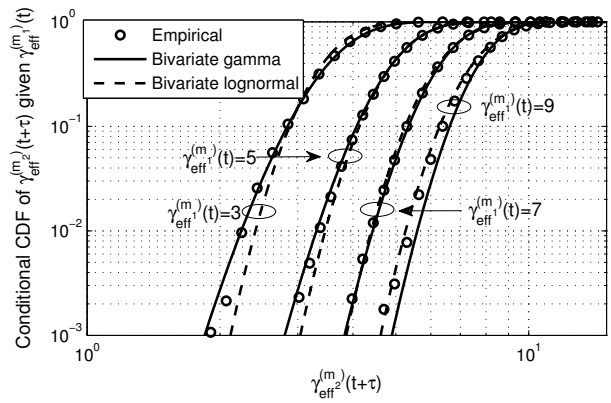


Fig. 1. Comparison of the conditional CDFs of EESM with the proposed bivariate gamma distribution for independent subcarriers ( $\sigma^2 = 10$  dB,  $N_{\text{sc}} = 12$ ,  $\beta_{m_1} = \beta_{m_2} = 5$ ,  $D = 2$  (SISO), and  $f_d\tau = 0.1$ ).

and the cross-correlation of  $Y_{m_1}(t)$  and  $Y_{m_2}(t + \tau)$  is

$$\begin{aligned} \mathbb{E}[Y_{m_1}(t)Y_{m_2}(t + \tau)] &= \frac{1}{N_{\text{sc}}^2} \sum_{i=1}^{N_{\text{sc}}} \sum_{j=1}^{N_{\text{sc}}} [(1 + 2a\beta_{m_1}^{-1}) \\ &\quad \times (1 + 2a\beta_{m_2}^{-1}) - 4\rho(\tau)a^2 |C_{ij}|^2 \beta_{m_1}^{-1} \beta_{m_2}^{-1}]^{-\frac{D}{2}}. \end{aligned} \quad (18)$$

*Proof:* The proof is relegated to Appendix B. ■

## B. Average Throughput Analysis

We are now in a position to evaluate  $\bar{R}(\tau)$  in (4) and derive the following novel expression for the average throughput.

**Result 2:** The average throughput as a function of feedback delay is given by (22) at the top of next page.

## IV. NUMERICAL RESULTS

### A. Empirical Verification of the Proposed Distribution

We first evaluate the accuracy of the proposed model by comparing its CDF with that obtained empirically. This approach is widely used in the wireless modeling literature [12], [21]. In our problem, the joint CDF plots are three-dimensional in nature. We, therefore, plot the conditional CDF of  $\gamma_{\text{eff}}^{(m_2)}(t + \tau)$  given  $\gamma_{\text{eff}}^{(m_1)}(t)$  for different values of  $\gamma_{\text{eff}}^{(m_1)}(t)$ , and compare it with that obtained from Monte Carlo simulations. We use the typical urban (TU) and the rural area (RA) channel profiles [22]. The number of terms required to accurately compute the infinite summation in (7) is 85 and 35 for independent subcarriers and TU channel, respectively.

Figure 1 compares the conditional CDFs for independent subcarriers for  $D = 2$  (SISO) and  $f_d\tau = 0.1$ . Notice that the bivariate gamma model tracks the empirical curves well over a range of values that span three orders of magnitude. Its accuracy is comparable to the bivariate lognormal model. While it is more accurate than the bivariate lognormal model for smaller values of  $\gamma_{\text{eff}}^{(m_1)}(t)$ , the reverse is true for larger values of  $\gamma_{\text{eff}}^{(m_1)}(t)$ .

Figure 2 plots the conditional CDFs for TU channel for  $D = 4$  ( $1 \times 2$  SIMO). Now, with correlated subcarriers, the proposed model is more accurate than the bivariate lognormal model. As mentioned before, corresponding results for the beta [15],

$$\begin{aligned} \bar{R}(\tau) \approx \sum_{m=1}^L r_m \left\{ \Gamma_{\text{inc}} \left( q_{m+1,m}, \frac{T_{m+1}}{s_{m+1,m}} \right) - \Gamma_{\text{inc}} \left( q_{m,m}, \frac{T_m}{s_{m,m}} \right) + \sum_{k=0}^{\infty} \left[ \frac{(\xi_{m,m})^{q_{m,m}} (1 - \xi_{m,m})^k}{kB(k, q_{m,m})} \right. \right. \\ \times \Gamma_{\text{inc}} \left( k + q_{m,m}, \frac{T_m p_{m,m}}{r_{m,m}} \right) \Gamma_{\text{inc}} \left( k + q_{m,m}, \frac{T_m s_{m,m}}{r_{m,m}} \right) - \frac{(\xi_{m+1,m})^{q_{m+1,m}} (1 - \xi_{m+1,m})^k}{kB(k, q_{m+1,m})} \\ \left. \left. \times \Gamma_{\text{inc}} \left( k + q_{m+1,m}, T_{m+1} \frac{p_{m+1,m}}{r_{m+1,m}} \right) \Gamma_{\text{inc}} \left( k + q_{m+1,m}, T_m \frac{s_{m+1,m}}{r_{m+1,m}} \right) \right] \right\}, \quad (22) \end{aligned}$$

where  $\xi_{m_1, m_2} = \frac{r_{m_1, m_2}}{s_{m_1, m_2} p_{m_1, m_2}}$ , for  $m_1, m_2 \in \{m, m+1\}$  and  $T_{L+1} = \infty$ .

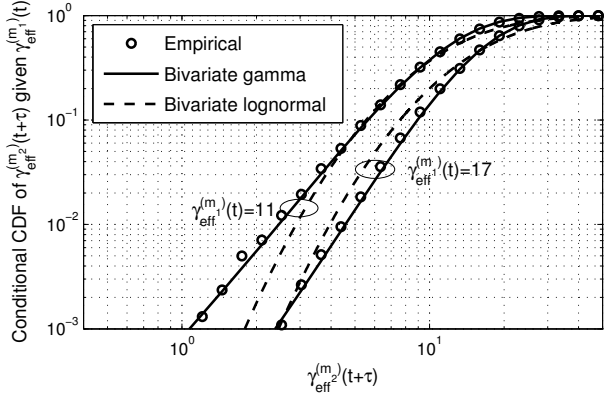


Fig. 2. Comparison of the conditional CDFs of EESM with the proposed bivariate gamma distribution for TU channel profile ( $\sigma^2 = 10$  dB,  $N_{\text{sc}} = 12$ ,  $\beta_{m_1} = \beta_{m_2} = 5$ ,  $D = 4$  ( $1 \times 2$ SIMO), and  $f_d \tau = 0.1$ ).

GEV, and Pearson [16] models cannot be shown because no tractable bivariate extension is known for them.

### B. Throughput

We now present Monte Carlo simulations to evaluate the accuracy of the throughput analysis. The MCSs specified in the LTE standard are used [17, Tbl. I]. We set  $\text{BLER}_t = 0.1$ ,  $N_{\text{sc}} = 24$ , and  $D = 2$  (SISO). The number of terms used to evaluate the infinite series in (22) depends on  $f_d \tau$  and the correlation between the subcarriers. For example, for  $f_d \tau = 0.1$ , 20 and 100 terms are sufficient for correlated and independent subcarriers, respectively.

The average throughput as a function of  $f_d \tau$  for different average SNRs  $\sigma^2$  is shown in Figure 3 for the RA channel. The corresponding plot for the TU channel is shown in Figure 4. Notice the good match between the analysis and simulations in both the figures. As  $f_d \tau$  increases, the average throughput decreases. We quantify it in terms of the percentage drop in throughput from  $f_d \tau = 0$  to 0.3. For  $\sigma^2 = 5$  dB, 10 dB, and 20 dB, the percentage drops respectively are 59%, 57%, and 54% in the RA channel, and 55%, 53%, and 46% in the TU channel. Thus, the drop in throughput due to feedback delay increases as the correlation between the subcarriers increases.

We now study the effect of the number of subcarriers on the throughput in Figure 5. We consider independent subcarriers with  $N_{\text{sc}} = 1, 12$ , and 24 since this was the worst case in terms of accuracy for the proposed bivariate EESM model. Note that for  $N_{\text{sc}} = 1$ , EESM-based AMC reduces to the classical

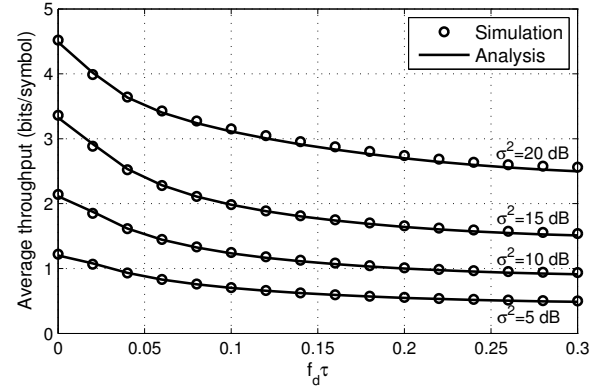


Fig. 3. RA channel: Average throughput as a function of normalized delay for different per-link average SNRs ( $N_{\text{sc}} = 24$  and  $D = 2$  (SISO)).

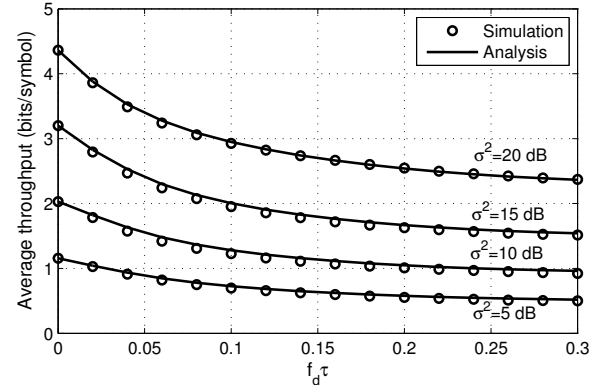


Fig. 4. TU channel: Average throughput as a function of normalized delay for different per-link average SNRs ( $N_{\text{sc}} = 24$  and  $D = 2$  (SISO)).

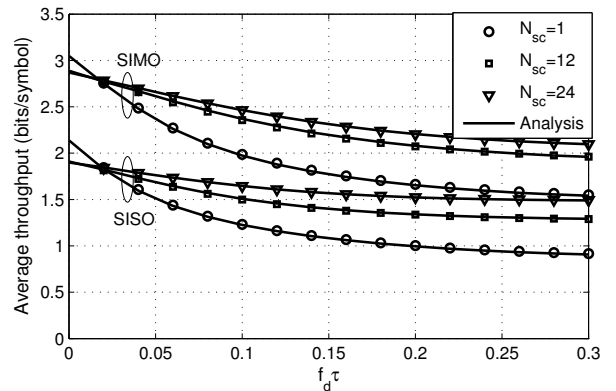


Fig. 5. Effect of number of subcarriers on average throughput as a function of normalized delay for independent subcarriers ( $\sigma^2 = 10$  dB).

narrowband AMC [1]. As the feedback delay increases, the throughput decreases more rapidly for  $N_{sc} = 1$  than for  $N_{sc} = 24$ . This is a consequence of the frequency diversity achieved by transmitting over multiple subcarriers. Notice again the good match between analysis and simulations.

## V. CONCLUSIONS

We presented a general analytical framework to characterize the impact of feedback delay on EESM-based link adaptation in frequency-selective channels. We first proposed a novel bivariate gamma distribution for the joint distribution of EESM at the times of MCS determination and data transmission. An MGF-matching method, which exploits the functional form of EESM, was used to compute the distribution's parameters. We saw that the proposed model is quite accurate for both independent and correlated subcarriers. It then led to a novel and accurate expression for the throughput as a function of feedback delay. Our analysis covered different multiple antenna modes and arbitrary subcarrier correlations. While feedback delays can significantly degrade the throughput, the diversity achieved by transmitting over multiple subcarriers or using multiple antennas partially mitigates it.

An avenue for future work is to incorporate co-channel interference and scheduling into the system model.

## APPENDIX

### A. Probability of Successful Transmission with MCS $m$

We replace the probability of successful transmission with MCS  $m$  in (3) with its upper bound:

$$P\left(\gamma_{\text{eff}}^{(m)}(t) \geq T_m, \gamma_{\text{eff}}^{(m+1)}(t) < T_{m+1}, \dots, \gamma_{\text{eff}}^{(L)}(t) < T_L, \right. \\ \left. \gamma_{\text{eff}}^{(m)}(t + \tau) \geq T_m\right) \approx P\left(\gamma_{\text{eff}}^{(m)}(t) \geq T_m, \right. \\ \left. \gamma_{\text{eff}}^{(m+1)}(t) < T_{m+1}, \gamma_{\text{eff}}^{(m)}(t + \tau) \geq T_m\right). \quad (23)$$

We simplify (23) further using the following lower bound:

$$P\left(\gamma_{\text{eff}}^{(m)}(t) \geq T_m, \gamma_{\text{eff}}^{(m+1)}(t) < T_{m+1}, \gamma_{\text{eff}}^{(m)}(t + \tau) \geq T_m\right) \\ \geq P\left(\gamma_{\text{eff}}^{(m)}(t) \geq T_m, \gamma_{\text{eff}}^{(m)}(t + \tau) \geq T_m\right) \\ - P\left(\gamma_{\text{eff}}^{(m+1)}(t) \geq T_{m+1}, \gamma_{\text{eff}}^{(m)}(t + \tau) \geq T_m\right). \quad (24)$$

Substituting (24) in (23) yields the desired result in (4).

### B. Moments of $Y_{m_1}(t)$ and $Y_{m_2}(t + \tau)$

The means of  $Y_{m_1}(t)$  and  $Y_{m_2}(t + \tau)$  are derived in [15]. Here, we derive the cross-correlation of  $Y_{m_1}(t)$  and  $Y_{m_2}(t + \tau)$  and the second moment. The cross-correlation is given by

$$\mathbb{E}[Y_{m_1}(t)Y_{m_2}(t + \tau)] = \frac{1}{N_{sc}^2} \sum_{i=1}^{N_{sc}} \sum_{j=1}^{N_{sc}} \mathbb{E}\left[e^{-\frac{\gamma_i(t)}{\beta_{m_1}} - \frac{\gamma_j(t+\tau)}{\beta_{m_2}}}\right] \\ = \frac{1}{N_{sc}^2} \sum_{i=1}^{N_{sc}} \sum_{j=1}^{N_{sc}} \Psi_{\gamma_i(t), \gamma_j(t+\tau)}(\beta_{m_1}^{-1}, \beta_{m_2}^{-1}). \quad (25)$$

The joint MGF of  $\gamma_i(t)$  and  $\gamma_j(t + \tau)$  is given by (8) with  $q = \frac{D}{2}$ ,  $s = 2a$ ,  $p = 2a$ , and  $r = 4a^2 \left(1 - \rho(\tau) |C_{ij}|^2\right)$ , which when substituted in (25) yields (18). Substituting  $\tau = 0$  in (18) yields the expression for the second moment in (17).

## REFERENCES

- [1] A. J. Goldsmith, *Wireless Communications*, 1st ed. Cambridge Univ. Press, 2005.
- [2] S. Sesia, I. Toufik, and M. Baker, *LTE – The UMTS Long Term Evolution, From Theory to Practice*, 1st ed. John Wiley and Sons, 2009.
- [3] S. Guharoy and N. B. Mehta, "Joint evaluation of channel feedback schemes, rate adaptation, and scheduling in OFDMA downlinks with feedback delays," *IEEE Trans. Veh. Technol.*, vol. 62, no. 4, pp. 1719–1731, May 2013.
- [4] A. Kuhne and A. Klein, "Throughput analysis of multi-user OFDMA-systems using imperfect CQI feedback and diversity techniques," *IEEE J. Sel. Areas Commun.*, vol. 26, no. 8, pp. 1440–1450, Oct. 2008.
- [5] S. Ye, R. S. Blum, and L. J. Cimini, "Adaptive OFDM systems with imperfect channel state information," *IEEE Trans. Wireless Commun.*, vol. 5, no. 11, pp. 3255–3265, Nov. 2006.
- [6] M. Goldenbaum, R. A. Akl, S. Valentin, and S. Stanczak, "On the effect of feedback delay in the downlink of multiuser OFDM systems," in *Proc. CISS*, Mar. 2011, pp. 1–6.
- [7] T. L. Jensen, S. Kant, J. Wehinger, and B. H. Fleury, "Fast link adaptation for MIMO OFDM," *IEEE Trans. Veh. Technol.*, vol. 59, no. 8, pp. 3766–3778, Oct. 2010.
- [8] K. Brueninghaus, D. Astely, T. Salzer, S. Visuri, A. Alexiou, S. Karger, and G.-A. Seraji, "Link performance models for system level simulations of broadband radio access systems," in *Proc. PIMRC*, Sep. 2005, pp. 2306–2311.
- [9] S. S. Tsai and A. C. K. Soong, "Effective-SNR mapping for modeling frame error rates in multiple-state channels," 3GPP2, Tech. Rep. 3GPP2-C30-20030429-010, 2003.
- [10] "Feasibility study for OFDM for UTRAN enhancement," 3GPP, Tech. Rep. 25.892 v2.0.0 (2004-06), 2004.
- [11] R. Srinivasan, J. Zhuang, L. Jalloul, R. Novak, and J. Park, "IEEE 802.16m evaluation methodology document (EMD)," Tech. Rep. IEEE 802.16m-08/004r2, 2008.
- [12] S. N. Donthi and N. B. Mehta, "An accurate model for EESM and its application to analysis of CQI feedback schemes and scheduling in LTE," *IEEE Trans. Wireless Commun.*, vol. 10, no. 10, pp. 3436–3448, Oct. 2011.
- [13] S. Simoens, S. Rouquette-Léveillé, P. Sartori, Y. Blankenship, and B. Clason, "Error prediction for adaptive modulation and coding in multiple-antenna OFDM systems," *Signal Process.*, vol. 86, no. 8, pp. 1911–1919, Aug. 2006.
- [14] T. Tao and A. Czylik, "Performance analysis of link adaptation in LTE systems," in *Proc. Int. ITG Workshop on Smart Antennas (WSA)*, Feb. 2011, pp. 1–5.
- [15] J. Francis and N. B. Mehta, "EESM-based link adaptation in point-to-point and multi-cell OFDM systems: Modeling and analysis," *IEEE Trans. Wireless Commun.*, vol. 13, no. 1, pp. 407–417, Jan. 2014.
- [16] H. Song, R. Kwan, and J. Zhang, "Approximations of EESM effective SNR distribution," *IEEE Trans. Commun.*, vol. 59, no. 2, pp. 603–612, Feb. 2011.
- [17] J. Fan, Q. Yin, G. Y. Li, B. Peng, and X. Zhu, "MCS selection for throughput improvement in downlink LTE systems," in *Proc. ICCCN*, Aug. 2011, pp. 1–5.
- [18] F. Chatelain, J.-Y. Tourneret, J. Inglada, and A. Ferrari, "Bivariate gamma distributions for image registration and change detection," *IEEE Trans. Image Process.*, vol. 16, no. 7, pp. 1796–1806, Jul. 2007.
- [19] I. S. Gradshteyn and I. M. Ryzhik, *Table of Integrals, Series and Products*, 4th ed. Academic Press, 1980.
- [20] V. Annapureddy, D. Marathe, T. R. Ramya, and S. Bhashyam, "Outage probability of multiple-input single-output (MISO) systems with delayed feedback," *IEEE Trans. Commun.*, vol. 57, no. 2, pp. 319–326, Feb. 2009.
- [21] G. L. Stüber, *Principles of Mobile Communications*. Kluwer Academic Publishers, 1996.
- [22] "Universal mobile telecommunications system (UMTS); deployment aspects," 3GPP, Tech. Rep. 25.943 v6.0.0 (2004-12), 2004.